

High resolution spectroscopy of symbiotic stars[★]

V. Orbital and stellar parameters for FG Ser (AS 296)

U. Mürset¹, T. Dumm¹, S. Isenegger¹, H. Nussbaumer¹, H. Schild¹, H.M. Schmid^{2,3}, and W. Schmutz^{1,4}

¹ Institut für Astronomie, ETH-Zentrum, 8092 Zürich, Switzerland

² Landessternwarte Heidelberg-Königstuhl, 69117 Heidelberg, Germany

³ Max-Planck-Institut für Astronomie, Königstuhl 17, 69117 Heidelberg, Germany

⁴ Physikalisch-Meteorologisches Observatorium, 7260 Davos, Switzerland

Received 30 June 1999 / Accepted 23 September 1999

Abstract. For the eclipsing symbiotic binary FG Ser (AS 296) we have obtained a series of high resolution optical spectra. Combining the measured radial velocity variations for the red giant with published eclipse photometry gives a binary period of 650 days. We derive the radial velocity curve of the red giant, yielding the orbital parameters of the system and a mass function of $m_f = 0.039 M_\odot$. We further determine the rotation velocity of the red giant, and assuming corotation derive its photospheric radius. Together with the spectral type surface temperature this yields the position of the red giant in the HR-diagram and a mass estimate of $M_c = 1.7 M_\odot$. Combining this value with m_f results in a mass of $M_h = 0.60 M_\odot$ for the hot star. With a binary separation of 1.95 AU and a radius of the red giant of $105 R_\odot$ we find that FG Ser is a detached binary with the red giant well inside the Roche lobe.

Key words: stars: binaries: spectroscopic – stars: binaries: symbiotic – stars: fundamental parameters – stars: individual: FG Ser – stars: individual: AS 296

1. Introduction

The knowledge of orbital and stellar parameters of interacting binary systems is fundamental for understanding their interaction processes. This is the fifth paper in a series that derives such parameters for southern symbiotic systems. In former papers we investigated SY Mus (Schmutz et al. 1994, Paper I), RW Hya (Schild et al. 1996, Paper II), CD–43.14304 (Schmid et al. 1998, Paper III), and BX Mon (Dumm et al. 1998, Paper IV). Here, we analyze our observations of FG Ser (= AS 296).

FG Ser has been known as a stellar emission line object since the time of Merrill & Burwell (1950). In June 1988 a strong outburst attracted renewed attention to FG Ser. Photometric data of

this event were presented by Munari & Whitelock (1989) and Munari et al. (1992, 1995). They observed that the outbursting object is eclipsed by the red giant in the system and derived an eclipse ephemeris $T_{\text{eclipse}} = 48492 + 658 \times E$ (Munari et al. 1995). The eclipses establish that we see FG Ser at high inclination so that we can make the helpful simplification $\sin i \approx 1$.

2. Observations

The high resolution data were collected between September 1991 and March 1996 at ESO in La Silla, Chile, in the course of a monitoring program of symbiotic stars. FG Ser was observed with the Coudé Echelle Spectrograph (CES) fed by the 1.4 m Coudé Auxilliary Telescope (CAT). A log of the observations is given in Table 1. The data were recorded with various CCDs. Most observations were carried out remotely from the ESO headquarters near Munich. The settings cover approximately 55 Å; they are centered at H α , $\lambda_c = 7005$ Å, and $\lambda_c = 7453$ Å. Further we have taken with the same instrument one spectrum of the Na I resonance line region for studying the interstellar absorption towards FG Ser. The spectral resolution of our CAT-spectra is $R \approx 100\,000$ for the 7453 Å setting and $R \approx 60\,000$ for the other settings.

The data reduction includes bias subtraction, flat field correction, spectrum extraction, a particularly careful wavelength calibration, and a rectification of the continuum. Further details are as described in Paper III.

3. The orbit of the cool giant

The spectra used for radial velocity measurements of the red giant in FG Ser are listed in Table 1. All these observations were complemented, without changing the instrumental setup, with an exposure of the radial velocity standard star HR4763, which according to Foster & Wall (1998) has $V_0 = 21.3 \pm 0.5 \text{ km s}^{-1}$. This allows us to derive by cross-correlation accurate radial velocities of the cool star's absorption spectrum. The results are given in Table 1. We estimate the uncertainty of these velocities at $\Delta v \approx 0.7 \text{ km/s}$. The settings at $\lambda_c = 7453$ Å have higher resolution, and we estimate $\Delta v \approx 0.5 \text{ km/s}$.

Send offprint requests to: H. Schild (hschild@astro.phys.ethz.ch)

[★] Based on observations obtained at the European Southern Observatory, La Silla, Chile; the observations were granted for the ESO programs 47.7-081, 48.7-083, 49.7-041, 50.7-129, 51.7-093, 52.7-068, 53.7-083, 54.E-061, 55.E-446, 56.E-526

Table 1. Log of observations for FG Ser. The phase φ is calculated from the orbit solution given in Table 2. RV is the measured barycentric radial velocity of the cool giant, and EW the H α emission line equivalent width.

Date	JD	φ	λ_c	RV [km s $^{-1}$]	EW [Å]
27-4-1991	48374*	0.82		63.4 ± 2.1	
11-9-1991	48511	0.03	7005	74.0 ± 0.7	
17-3-1992	48699	0.32	6563	77.7 ± 0.7	161.4
15-5-1992	48758	0.41	6563	74.9 ± 0.7	173.1
28-7-1992	48832	0.53	6563	69.1 ± 0.7	148.6
25-5-1993	49133	0.99	6563	69.9 ± 0.7	119.7
14-5-1994	49487	0.53	6563	70.6 ± 0.7	134.3
17-7-1994	49551	0.63	6563	66.0 ± 0.7	171.8
20-5-1995	49858	0.10	6563	76.5 ± 0.7	125.4
14-9-1995	49975	0.28	7453	80.1 ± 0.5	
5-3-1996	50148	0.55	7453	68.1 ± 0.5	
25-5-1993	49133	0.99	5885		

* from Wallerstein et al. (1993)

We complement our own measurements with a value from Wallerstein et al. (1993) based on red giant absorption features. They also quote further RV measurements from the early outburst phase which, however, are not directly related to the red giant. These values scatter strongly from one ionic species to the other probably because of dynamical gas motions during the outburst. We disregard these early measurements.

Our radial velocity data cover 2.7 orbital cycles. In order to find the orbital parameters P , T_0 , K , V_0 , e and ω , we performed a least squares fitting procedure (cf. Paper I). Table 2 gives the best solutions. The best fit leaving all 6 orbital parameters free (column (1) of Table 2) results in a small eccentricity of $e = 0.11$. However this small value of e differs not significantly from $e = 0$. An eccentric orbit is also not expected for FG Ser as the theory of tidal interaction for stars with a fully convective envelope (Zahn 1977, and Paper I) predicts a circularisation of the binary orbit, $e = 0$, on a timescale of the order of 10^6 years. This is short compared to the timescale of the hydrogen shell-burning phase in low mass stars which is according to Vassiliadis & Wood (1993) of the order of 10^8 years. For this reason we prefer a fit solution where the eccentricity is forced to be $e = 0$.

As our radial velocity curve is based on a relatively small data set we also consider the constraints on the orbital motion from photometric eclipse observations. Eclipses of the hot component in FG Ser are only seen during outburst and the corresponding light curves include not only eclipses but also strong intrinsic variations of the hot component. Fortunately, there exists in the data of Munari et al. (1992) a well defined minimum for 1991 which is useful for determining the exact conjunction phase T_0 . Fig. 1 shows the V magnitudes of the 1991 eclipse in two different ways: 1) as published, and 2) as mirrored at various T_0 . For $T_0 = 48491$ we find mirrored values that fit best the original ones. For $T_0 = 48493$ the mirrored values lag behind the original ones, and vice versa for $T_0 = 48489$. We adopt $T_0 = 48491 \pm 1$. This value is compatible with the ephemeris

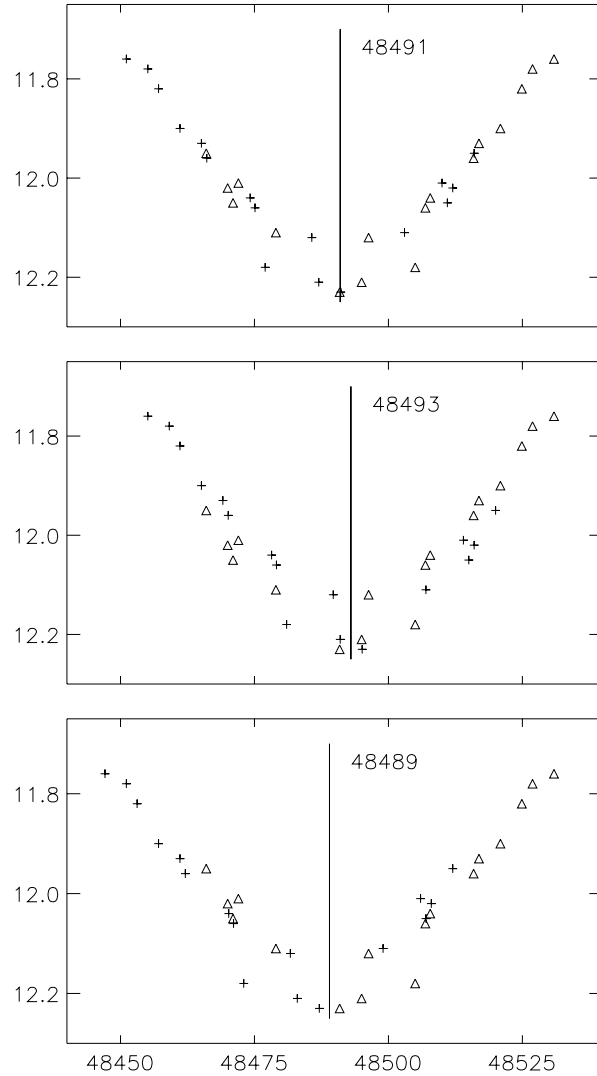


Fig. 1. V-magnitudes during the central part of the 1991 eclipse. Triangles show the values published by Munari et al. (1992). Crosses are the same values “mirrored” at the indicated dates. In the lower two panels the mirrored magnitudes are systematically shifted against the non-mirrored ones. The top panel shows the best estimate for mid-eclipse.

of Munari et al. (1995; $T_0 = 48492 \pm 4$), however, we adopt a narrower error bar. The photometric T_0 -value differs by 7 days from the value obtained with a zero-eccentricity fit to our radial velocity data. As the quality of the mid-eclipse T_0 -determination seems to be high we finally opt for the radial velocity solution, where e and T_0 are pre-fixed to $e = 0$, and $T_0 = 48491$. The resulting orbital period is then $P = 650 \pm 5$ days. In the following we will use the orbital parameters from this solution. The corresponding radial velocity curve is plotted in Fig. 2.

Our procedure assumes that the light curve is symmetrical to mid-eclipse. An asymmetrical eclipse light curve is observed in SY Mus. Dumm et al. (1999) interpret that observation as indication of an asymmetrical density distribution around the M-giant. Should FG Ser have a similar configuration then the

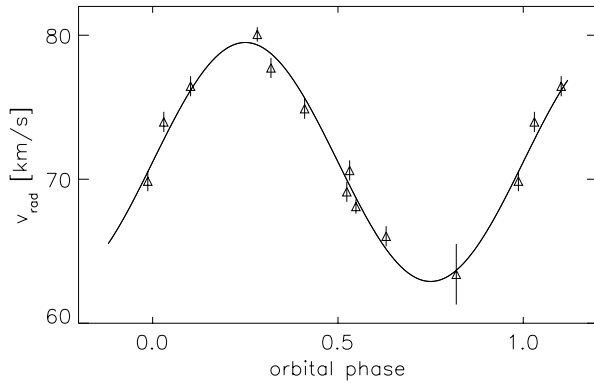


Fig. 2. Radial velocity curve of FG Ser. The phases and velocities are calculated according to the adopted solution (Table 2). The three left-most points are repeated on the right.

Table 2. Orbital solutions for the cool giant. P : binary period, T_0 : date when the red giant is in front of the hot component ($\varphi = 0$) or date of periastron passage; K : radial velocity semi-amplitude; V_0 : system radial velocity; e : eccentricity; ω : angle of periastron; $\sigma_v = \frac{1}{n} \sqrt{\sum \Delta v^2}$. Column (1) gives the best overall fit, (2) best fit that reproduces the ephemeris of Munari et al. (1995). Underlined values are pre-fixed (see text).

Parameter	Least squares fit solutions		
	(1)	(2)	adopted
P [d]	655	<u>658</u>	650 ± 5
T_0 [JD]	48497	<u>48492</u>	<u>48491</u> ± 1
T_P [JD]	48557	48656	
K [km s $^{-1}$]	8.6	8.1	8.3 ± 0.2
V_0 [km s $^{-1}$]	71.3	71.4	71.2 ± 0.2
e	0.11	0.06	<u>0</u> $+ 0.2$
ω	311 $^\circ$	8 $^\circ$	—
m_f [M_\odot]	0.043	0.036	0.039 ± 0.004
σ_v [km s $^{-1}$]	0.18	0.25	0.24

uncertainty in T_0 and P could be larger than indicated above or in Table 2.

We note that the period of Munari et al. (1995), based on the few observable eclipses, is somewhat longer but still has overlap in the error bars with our determination. For completeness we give in Table 2 also the best fit parameters obtained from the pre-fixed P - and T_0 -values from the ephemeris of Munari et al. (1995).

4. Parameters of the red giant

The red giant in FG Ser is classified as spectral type M5 (Mürset & Schmid 1999). According to the scale by Dyck et al. (1996) this corresponds to an effective temperature $T_c = (3470 \pm 100)$ K. The error estimate includes an uncertainty in the spectral type of 1 M-subclass. The typical radius of an M5-giant is 100–150 R_\odot according to a statistical study of M giants in the solar vicinity (Dumm & Schild 1998).

A direct determination of the radius of the red giant in FG Ser can be made with a rotation velocity measurement. The method

assumes that co-rotation has been established for the red giant. This assumption is justified by theoretical estimates on tidally induced co-rotation, and is probably valid for most s-type symbiotics as already outlined in Paper I (see also Zahn 1977).

We derive the projected rotation velocity $v_{\text{rot}} \cdot \sin i$ of the cool giant from the absorption lines in the spectra centered at 7453 Å. The method determines the rotational broadening of weak absorption lines with respect to a template spectrum of a non-rotating comparison star (see Paper IV for details). We find $v_{\text{rot}} \cdot \sin i = 8 \pm 1$ km/s. Since FG Ser is an eclipsing system we set $\sin i = 1$ and assume further that the tidal forces responsible for co-rotation have also aligned the stellar and orbital rotational axes. The red giant's radius is then given by

$$R_c = \frac{P \cdot v_{\text{rot}}}{2\pi} = (105 \pm 15) R_\odot. \quad (1)$$

This is compatible with the statistical values from the work of Dumm & Schild (1998). The luminosity that follows from R_c and the spectral type temperature is $L_c = (1440 \pm 600) L_\odot$.

We now compare the derived luminosity and temperature with theoretical evolutionary tracks in the HR-diagram. It seems that the cool star in FG Ser is on the first giant branch, because the giant shows in the IR no, or at most very little variability ($K = 4.46 \pm 0.03$ Kenyon 1988, see also Munari et al. 1995). Further there is no dust emission visible in the system. Both properties, variability and strong dust emission, are typical for cool AGB giants, and their absence in FG Ser provides evidence that the cool component is on the first giant branch. From the RGB evolutionary tracks for solar abundances of Bessell et al. (1989) we find an initial mass $M_c = (1.8 \pm 0.6) M_\odot$ for the cool giant. FG Ser is a high velocity object that probably belongs to the old disk population (Brugel & Wallerstein 1981). It could thus have a metallicity that is lower than solar, although a metallicity far below solar can be excluded because the absorption lines in the red giants spectrum have normal strength. If we use the tracks of Vassiliadis & Wood (1993) for a metallicity $Z = 0.008$, we obtain for the red giant's mass $1.5 M_\odot$. The effect of metallicity on the mass is small and we adopt as the most likely value $M_c = (1.7 \pm 0.7) M_\odot$. Even AGB tracks (Bressan et al. 1993) are compatible with this range. The mass lost during its previous evolution from the main sequence to the red giant phase is most probably much smaller than the quoted error in the mass estimate. We therefore also adopt $M_c = (1.7 \pm 0.7) M_\odot$ as the current value for the cool giant.

5. The hot component and the binary geometry

From the orbital parameters of the cool giant we compute the mass function

$$m_f = \frac{1}{2\pi G} P K^3 (1 - e^2)^{3/2} = \frac{(M_h \cdot \sin i)^3}{(M_h + M_c)^2} \quad (2)$$

where M_h and M_c are the masses of the hot and the cool component, i is the orbit inclination, G the gravitational constant, P the period, and e the eccentricity. The FG Ser system is eclipsing and the binary inclination has to be high. From our orbital

parameters and the size of the red giant from Sect. 4 it follows that the inclination needs to be larger than 75° for an eclipse to occur. This uncertainty in i introduces an error of at most 5% in M_h . For all the solutions discussed above we find approximately $m_f = 0.04 M_\odot$. With $M_c = (1.7 \pm 0.7) M_\odot$ we obtain $M_h = 0.60 \pm 0.15 M_\odot$ for the mass of the hot companion (the error taking into account the uncertainties in M_c , m_f , and $\sin i$). The total system mass is $M_h + M_c = (2.3 \pm 0.9) M_\odot$ and the mass ratio is $M_c/M_h = 2.8 \pm 0.6$. The error in the ratio is relatively small because the masses are not independent. Kepler's third law yields a binary separation of approximately 2 AU. Our results are summarized in Table 3.

The distance from the center of the cool giant to the inner Lagrangian point L_1 is 2.4 times the radius of the giant. This fits into the picture of Mürset & Schmid (1999) who find that in symbiotic systems this ratio is often close to 2. The distance from L_1 to the surface of the red giant shows that FG Ser is a well detached system. This agrees with the conclusion of Munari et al. (1995) based on an analysis of the light variation.

Knowing the orbit and the size of the red giant we now revisit the eclipse light curve. The duration of the eclipse centered at JD 48491 was (110 ± 10) days from first to last contact. In the case of a purely geometrical, central occultation of a point source by the photosphere of radius R_c we expect an occultation length of only about 55 d. We thus conclude that the radius of the eclipsed light source (the secondary or an emission nebula) must have roughly the same size as the red giant ($\approx 120 R_\odot$). However, this conclusion has to be considered cautiously because in symbiotic systems absorption and scattering processes by circumstellar matter, especially in the orbital plane, may play an important role (e.g. Isliker et al. 1989; Schmid 1997) and mimic extended eclipses.

6. The distance

The known radius of the red giant opens the way for a reliable distance determination. From the surface brightness relation for M-giants given in Schild et al. (1999) we derive a distance

$$d = R_c \cdot 10^{7.96+0.33 \cdot K-0.13 \cdot J} = (1.1 \pm 0.2) \text{ kpc} \quad (3)$$

where we entered the K and J magnitudes from Kenyon (1988). We neglect the influence of interstellar reddening because the formula is rather insensitive to extinction.

An independent distance estimate is possible from the line profiles of the interstellar Na I $\lambda\lambda 5890, 5896$ absorption doublet. According to the map of Brand & Blitz (1993) the interstellar matter in the direction of FG Ser is receding. We therefore measure the greatest red-shift. We find absorptions up to a red shift of $v_{\text{LSR}} \approx 20$ km/s. The red edge of the absorption trough is, unfortunately, blended by an emission component. Therefore, our measurement is not very accurate. Comparison with Brand & Blitz yields $d \approx 1.5$ kpc, roughly in agreement with the distance derived from the giant's radius.

In addition, the Na I doublet shows absorption troughs with much larger red-shifts than found in the map of Brand & Blitz (1993). These components are probably not of interstellar ori-

Table 3. Summary of the parameters derived for the FG Ser system.

Parameter	Adopted	Uncertainty
<u>System parameters:</u>		
Distance d [kpc]	1.1	0.2
Period P [d]	650	5
Eccentricity e	0	< 0.2
Separation a [AU]	1.95	0.2
Mass function m_f [M_\odot]	0.039	0.004
Total mass [M_\odot]	2.3	0.9
Mass ratio	2.8	0.6
<u>Cool component:</u>		
Mass M_c [M_\odot]	1.7	0.7
Radius R_c [R_\odot]	105	15
Effective Temperature T_c [K]	3470	100
Luminosity L_c [L_\odot]	1440	600
<u>Hot component:</u>		
Mass M_h [M_\odot]	0.60	0.15

gin. In fact, their position is centered at the velocity of the system, with a width of approximately 50 km/s. Similar absorption features at a velocity of 65 km/s were already noticed by Wallerstein et al. (1993). By coincidence, our Na I observation was performed during eclipse ($\varphi = 0.99$). Hence, the center of the absorption has the same radial velocity as both stellar components. The width of the absorption is much too large to be compatible with interstellar absorption in the direction of FG Ser. The blue half of this trough ($v_{\text{rad}} = 45$ km/s ... 70 km/s) could, in principle, be due to an outflow from the system. However, we do not see a reasonable explanation for the red half.

7. H α emission

Fig. 4 shows the H α emission line profiles of FG Ser at various orbital phases. The spectra are ordered according to their orbital phase, however, they are collected from more than one cycle. The profiles show two peaks, a red shifted and a blue shifted one. The red peak is much stronger than the blue one, except around phase $\varphi \approx 0.2 \pm 0.1$. We note that there is no indication of a change in the H α line shape during eclipse ($\varphi = 0.99$). At first glance it is not clear whether we see a broad emission with absorption, or several shifted emission features.

In this work we concentrate on the determination of stellar and orbital parameters, and we therefore will not discuss the Balmer profiles in detail. We refer to a discussion in Schwank et al. (1997) where the formation of Balmer profiles in symbiotics was discussed. They found that the Balmer emission is formed close to the recombination zone which separates the H $^+$ from the H 0 region close to the red giant. The line profiles strongly depend on the velocity gradient of the expanding wind close to that recombination boundary. Schwank et al. (1997) conclude: "Whereas observed profiles might suggest two gas streams, or wind components of possibly similar velocities in different directions, our model calculations show that self-

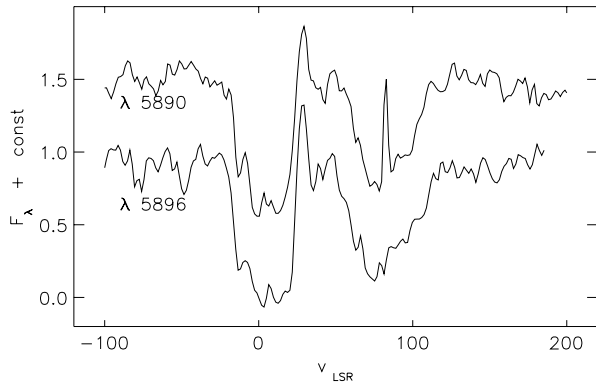


Fig. 3. Na I absorption profiles shifted to the local standard of rest.

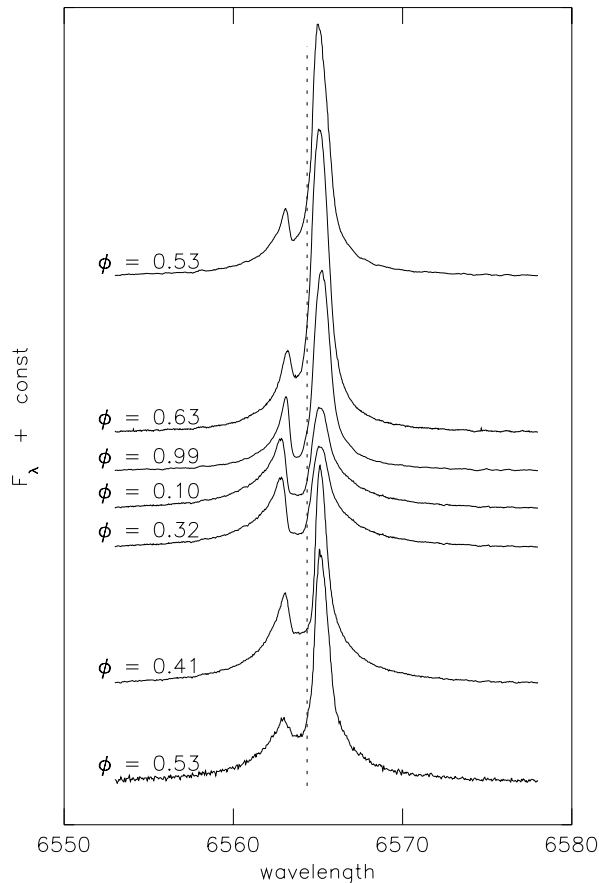


Fig. 4. Evolution of the H α line profiles. The profiles are shifted vertically for better display. They are corrected for the motion of the earth. The dotted line is the central wavelength of H α when shifted to the center of mass velocity of FG Ser.

absorption within an accelerating wind might be a more natural explanation.”

8. Conclusions

With this paper FG Ser enters the list of symbiotic objects with known orbital parameters. It turns out that at least as far as the orbital characteristics are concerned, FG Ser is an absolutely

Table 4. Masses of the stellar components in symbiotic binary systems.

Object	M_c/M_\odot	M_h/M_\odot	Reference
AX Per	1.0	0.4	Mikołajewska & Kenyon (1992)
EG And	1.5 ± 0.6	0.4 ± 0.1	Vogel et al. (1992)
AG Peg	2.6 ± 0.4	0.65 ± 0.10	Kenyon et al. (1993)
SY Mus	1.3 ± 0.25	0.43 ± 0.05	Paper I
RW Hya	1.6 ± 0.3	0.48 ± 0.06	Paper II
BX Mon	3.7 ± 1.9	0.55 ± 0.26	Paper IV
FG Ser	1.7 ± 0.7	0.60 ± 0.15	this work

“average” symbiotic: The period is typical for s-type objects, there is at most very little eccentricity, and the system is well detached. With the masses of $M_c = 1.7 M_\odot$ for the cool star and $M_h = 0.60 M_\odot$ for the white dwarf FG Ser fits well into the Table of stellar masses determined for symbiotic binaries so far (Table 4). It appears that most symbiotic systems have comparable masses, with a mass ratio of the order ~ 3 .

The average mass of the hot component in the symbiotic systems of Table 4 is $(0.50 \pm 0.04) M_\odot$ which is below the canonical value for single white dwarfs. For binaries with periods of a few hundred days, Li & van den Heuvel (1997) argue that for the white dwarf to become a Ia supernova, an initial minimum mass $M_h \sim 1.2 M_\odot$ is required. According to this scenario, the symbiotics in Table 4 are thus unlikely to suffer a SN event.

Acknowledgements. We are indebted to the ESO staff at Garching and La Silla who made the remote observations possible. TD acknowledges financial support by the Swiss National Science Foundation, and HMS by the Deutsche Forschungsgemeinschaft.

References

- Bessell M.S., Brett J.M., Scholz M., Wood P.R., 1989, A&AS 77, 1
 Brand J., Blitz L., 1993, A&A 275, 67
 Bressan A., Fagotto F., Bertelli G., Chiosi C., 1993, A&AS 100, 647
 Brugel E.W., Wallerstein G., 1981, The Observatory 101, 164
 Dumm T., Schild H., 1998, NewA 3, 137
 Dumm T., Mürset U., Nussbaumer H., et al., 1998, A&A 336, 637 (Paper IV)
 Dumm T., Schmutz W., Schild H., Nussbaumer H., 1999, A&A, in press
 Dyck H.M., Benson J.A., van Belle G.T., Ridgway S.T., 1996, AJ 111, 1705
 Foster K.W., Wall J., 1998, The Astronomical Almanac
 Isliker H., Nussbaumer H., Vogel M., 1989, A&A 219, 271
 Kenyon S.J., 1988, AJ 96, 337
 Kenyon S.J., Mikołajewska J., Mikołajewski M., Polidan R.S., Slovak M.H., 1993, AJ 106, 1573
 Li X.-D., van den Heuvel E.P.J., 1997, A&A 322, L9
 Mikołajewska J., Kenyon S.J., 1992, AJ 103, 579
 Merrill P.W., Burwell C.G., 1950, ApJ 112, 72
 Munari U., Whitelock P.A., 1989, MNRAS 239, 273
 Munari U., Whitelock P.A., Gilmore A.C., et al., 1992, AJ 104, 262
 Munari U., Yudin B.F., Kolotilov E.A., Gilmore A.C., 1995, AJ 109, 1740
 Mürset U., Schmid H.M., 1999, A&AS 137, 473

- Schild H., Mürset U., Schmutz W., 1996, A&A 306, 477 (Paper II)
- Schild H., Dumm T., Folini D., Nussbaumer H., Schmutz W., 1999, Proceedings of the Conference "The Universe as seen by ISO", ESA SP-427, 397
- Schmid H.M., 1997, in Physical Processes in Symbiotic Binaries and Related Systems, ed. J. Mikołajewska, Copernicus Found. for Polish Astron., Warsaw, p. 21
- Schmid H.M., Dumm T., Mürset U., et al., 1998 A&A 329, 986 (Paper III)
- Schmutz W., Schild H., Mürset U., Schmid H.M., 1994, A&A 288, 819 (Paper I)
- Schwank M., Schmutz W., Nussbaumer H., 1997, A&A 319, 166
- Vassiliadis E., Wood P.R., 1993, ApJ 413, 641
- Vogel M., Nussbaumer H., Monier R., 1992, A&A 260, 156
- Wallerstein G., Gilroy K.K., Willson L.A., Garnavich P., 1993, PASP 105, 859
- Zahn J.-P., 1977, A&A 57, 383